Siegel, R., and J. M. Savino, "An Analysis of the Transient Solidification of a Flowing Warm Liquid on a Convectively Cooled Wall," *Proc. 3rd Intern. Heat Transfer Conf.*, Vol. 4, pp. 141-151, Chicago, Ill. (1966).
Stephan, K., "Influence of Heat Transfer on Melting and Solidification in Forced Flow," *Intern. J. Heat Mass Transfer*, **12**, 199 (1969).
———, and B. Holzknecht, "Wärmeleitung beim Erstarren geometrisch einfacher Körper," *Wärme-und Stoffübertragung*, **7**, 200 (1974).
———, "Die asymptotischen Lösungen für Vorgänge des Erstarrens," *Intern. J. Heat Mass Transfer*, **19**, 597 (1976).
Tao, L. C., "Generalized Numerical Solutions of Freezing a Saturated Liquid in Cylinders and Spheres," *AIChE J.*, **13**, 165 (1967).

Manuscript received December 6, 1976; revision received September 27, and accepted October 12, 1977.

Droplet Size Spectra Generated in Turbulent Pipe Flow of Dilute Liquid/Liquid Dispersions

A. J. KARABELAS
Westhollow Research Center
Shell Development Company
P.O. Box 1380
Houston, Texas 77001

Experiments were carried out with water dispersed in hydrocarbons at various flow rates. The measured size spectra can be well represented by either an upper limit log-probability function or a Rosin-Rammler type of equation with constant parameters and only one variable, the maximum drop diameter d_{max} or d_{95}. The latter can be predicted satisfactorily by a correlation based on the Hinze/Kolmogorov model of droplet breakup.

SCOPE

Reliable estimates of the distribution of droplet sizes in flowing liquid/liquid dispersions are required in many areas of chemical engineering practice, for example, in the design of chemical reactors and of physical separation processes. At present, it is impossible to make such a priori estimates even in common problems, including pipe flow of dilute dispersions, owing to insufficient information about the effect of flow conditions on the size spectrum.

Collins and Knudsen (1970) have published the only available drop size distribution data, obtained in well-defined turbulent pipe flow with water as the continuous phase. These authors reached a rather disturbing conclusion, namely, that their data did not conform to any of the presently available distribution functions, such as the log-normal, upper limit log-normal, etc. In order to interpret the measured size spectra, Collins and Knudsen developed a computer aided stochastic model by postulating a breakup mechanism in which the maximum stable drop size d_{max} is a basic input parameter. However, the presently available correlations due to Hinze (1955) and Sleicher (1962) predict maximum droplet sizes d_{max}, in turbulent pipe flow, which differ almost by an order of magnitude for flow conditions and liquid properties of practical interest. Moreover, according to the Hinze model, d_{max} is approximately inversely proportional to the mean velocity $\overline{U}$, whereas in the Sleicher correlation, d_{max} varies with $\overline{U}^{-2.5}$. It is clear, therefore, that in the problem considered here, the literature provides very little guidance of questionable reliability.

The need to describe dispersions of water in flowing hydrocarbons provided the motivation for this work. The main objective was to make accurate measurements of droplet size spectra generated in turbulent pipe flow. In the absence of a satisfactory theory, such measurements are necessary in order to select the most representative distribution function and to study the influence of flow conditions and liquid properties on some physically significant parameters of the size spectrum, for example, the Sauter mean $\overline{d}_{32}$ or the maximum droplet diameter d_{max}.

CONCLUSIONS AND SIGNIFICANCE

Accurate data of water drop size spectra have been obtained by a relatively new droplet encapsulation technique. Two liquid hydrocarbons of viscosity approximately 2 and 20 mN s/m^2 have been used as the continuous phase in a 5.04 cm ID pipe loop with a straight test section 32 m long. The measured spectra show a remarkable similarity and can be satisfactorily represented by either an upper limit log-probability function or a Rosin-Rammler type of equation with nearly constant parameters (see Tables 2 and 4), the only variable being the characteristic size d_{max} or d_{95}. The latter can be predicted independently as a function of flow conditions and liquid physical properties.

The maximum drop sizes, or d_{95}, appear to be approximately inversely proportional to the mean flow velocity, in agreement with the theory of Kolmogorov (1949) and Hinze (1955). A correlation proposed by the latter author, essentially untested so far for pipe flow of dilute dispersions, has been reexamined and slightly modified to improve its accuracy at high Reynolds numbers. Our data are generally in good agreement with this correlation

0001-1541-78-9955-0170-$1.35

[Equation (23)]. Additional data (Kubie and Gardner, 1977) that became available after this paper was submitted for publication are also in agreement with this correlation.

In general, the data reported in this paper help delineate the basic features of drop size spectra in pipe flow and are expected to provide guidance in future modeling studies. For engineering calculations in particular, the results of this study suggest that the drop size spectrum can be estimated by using the Rosin-Rammler equation with a constant slope $n \simeq 2.5$ and with d_{95} computed from Equation (23).

PREVIOUS WORK

Basic studies of droplet breakup in homogeneous and isotropic turbulent flow were first presented by Kolmogorov (1949) and Hinze (1955). The main assumption in these studies is that drop fragmentation is caused by dynamic pressure forces, due to rapid turbulent fluctuations in the vicinity of the drops, which overcome interfacial tension forces. The mean square of velocity fluctuations $\overline{u^2}$, over a distance equal to the drop diameter d, provides a measure of the dynamic pressure forces. Therefore, an estimate of the maximum stable drop diameter $d_{\max}$ can be obtained from the condition

$$\frac{\rho_c \overline{u^2}}{2} = C' \frac{4\sigma}{d_{\max}} \tag{1}$$

For an isotropic and homogeneous flow field, it has been shown that $\overline{u^2}$ is proportional to $(\epsilon d)^{2/3}$ if the length d is much greater than the Kolmogorov microscale $\eta = (\nu^3/\epsilon)^{1/4}$. It follows that

$$d_{\max}\left[\frac{\rho_c}{\sigma}\right]^{3/5} \epsilon^{2/5} = C \tag{2}$$

where the constant C must be determined from experimental data. Hinze (1955) interpreted data taken by Clay (1940) in a Couette flow field and obtained the value $C = 0.725$ corresponding to d_{95}. The main assumptions made in the derivation of Equation (2) are, of course, open to criticism. For instance, turbulent shear fields of practical interest are far from isotropic and homogeneous. Nevertheless, Equation (2) has been found to describe quite satisfactorily experimental data obtained in agitated vessels; see, for example, Mlynek and Resnick (1972), Shinnar (1961), and Sprow (1967).

In order to estimate $d_{\max}$ or d_{95} in pipe flow, the mean rate of energy dissipation per unit mass of fluid $\bar{\epsilon}$ may be used

$$\bar{\epsilon} = \frac{2f\overline{U}^3}{D} \tag{3}$$

with the friction factor calculated from the Blasius equation for smooth pipes

$$f = \frac{0.0791}{Re^{1/4}} \tag{4}$$

and the constant $C = 0.725$ obtained in Couette flow. The result is

$$\frac{d_{95}}{D} = 1.516\left[\frac{\sigma}{D\rho_c\overline{U}^2}\right]^{0.6} Re^{0.10} \tag{5}$$

where $We = (D\rho_c\overline{U}^2)/(\sigma)$ is a dimensionless Weber number based on the pipe diameter D and mean velocity $\overline{U}$. Equations (2) and (5) will be reexamined in this paper and compared with data obtained in our study.

Sleicher (1962) made measurements of $d_{\max}$ in a relatively short test section of 3.81 cm ID which were not in agreement with predictions based on Equation (5). A transient type of technique was employed in these tests; that is, large drops of equal size were first introduced into the pipe when the flow rate was very small, and then the flow was accelerated, very fast, to the desired higher level. It was considered that the maximum stable diameter $d_{\max}$ had been obtained when less than 20% of the photographed drops had diameters smaller than the original size. Data obtained by Collins (1967) suggest that the line length used in this study may have been insufficient (6.7m or 176 pipe diameters of fully developed flow) for the large drops to reach a stable maximum size.

Sleicher took into account viscous forces and correlated his data by the following expression

$$\left[\frac{d_{\max}\rho_c\overline{U}^2}{\sigma}\right]\left[\frac{\mu_c\,\overline{U}}{\sigma}\right]^{1/2} = 38\left[1 + 0.7\left(\frac{\mu_d\,\overline{U}}{\sigma}\right)^{0.7}\right] \tag{6}$$

which is very different from Equation (5). For instance, it suggests that $d_{\max}$ is independent of pipe diameter, which is in sharp contrast to the $D^{0.5}$ dependence of Equation (5). Paul and Sleicher (1965) published later a few data points taken in a 1.27 cm ID pipe, which showed only a slight diameter effect ($d_{\max} \propto D^{-0.1}$). The constant $C = 43$ in Equation (6) gave a better fit of these data than $C = 38$. In subsequent calculations with this equation, the value $C = 40$ will be used.

Levich (1962) provides an interesting discussion of drop fragmentation mechanisms in his book and reviews related Russian work. He points out that the Kolmogorov model can give good estimates of stable drop diameters in the core of turbulent pipe flow but not in the region close to the wall. In this region of large velocity changes, much smaller drops will develop, with the smallest drop size to be found at the edge of the sublayer where

$$d_{\text{wall}} \simeq 2\left[\frac{\sigma\nu_c}{25\rho_c u_*^3}\right]^{1/2} \tag{7}$$

Obviously, during the transient period of dispersion formation in a pipe, the drop diameter will vary between a maximum, possibly given by the Kolmogorov-Hinze model for the core, and a minimum resulting from fragmentation at the wall, as suggested by Levich. At present, it is impossible to predict the equilibrium drop size distribution as a function of flow conditions and liquid physical properties, and accurate experiments are necessary to gain some insight into this problem.

Collins and Knudsen (1970) have published the only available drop size distribution data,* obtained in a 11.3

* After this paper was submitted for publication, a similar study was published by Kubie and Gardner (1977). These authors, using a photographic technique, measured drop size spectra but made no attempt to correlate them. They did conclude, however, that the measured maximum drop sizes were in good agreement with the Hinze correlation [Equation (5)].

m long, 1.89 cm ID pipe. The dispersion of three organic liquids in water was studied at relatively high velocities (4.3 to 6.1 m/s). Drop size distributions were obtained from photographs. For the prediction of d_{max}, Collins and Knudsen (1967, 1970) preferred the Sleicher correlation, although they did not systematically compare their data to existing models. In order to explain the measured drop size distributions, they developed a computer-aided stochastic model in which d_{max} is a basic input parameter. Owing to their significance, some of Collins' data will be reexamined and compared with the results of this study in the Appendix. In the following sections we shall first describe our experiments and then present and interpret the data.

DESCRIPTION OF EXPERIMENTS

Flow Loop

A schematic of the flow system is shown in Figure 1. The test section was made of acrylic pipe sections, with very smooth joints, and had a total length of ~32.3 m. The true inner diameter was 5.04 cm. Fluid was circulated by a rotary type of pump (manufacturer Bowie Company, 500 series). A Schroeder LF-I in-line filter (No. 2, Figure 1) was installed at the discharge end of the pump to remove small particles or droplets. A pressure relief diaphragm (3) and a pulsation dampener (4) were necessary to protect the pipe against pressure surges and to eliminate flow pulsations, respectively. A calming section (5), made of a 15 cm ID pipe, served the dual purpose of disengaging gas bubbles from the fluid and providing a uniform stream into the main line.

A special water injection facility (6) was used. Water was released at a steady rate (5 to 12 cm^3/s) into the main stream, through a 6 mm steel tube. Under these conditions, that is, low relative jet velocity and fairly large jet diameter, it is expected that the jet breakup is controlled almost entirely by the turbulence in the main stream. Moreover, it is reasonable to expect that the largest droplets developing upon disintegration of this jet are greater than the ultimate maximum stable diameter generated by the pipe flow; that is, the process of breakup continues downstream of the injection tube. Experiments by Collins (1967) with similar injection tubes, and larger main flow velocities than those of our experiments, show exactly this trend.

Pictures of the flowing dispersion were taken at a special test section (7), and samples were withdrawn simultaneously through a short 1.14 cm ID tube, located approximately 29 and 30 m, respectively, downstream of the injection point. The center line of the sampling tube was approximately 1.45 cm below the pipe center line.

A Halliburton turbine meter (12) was used to monitor the flow rate. Two large steel tanks were employed. One of them (14) was connected to the suction side of the pump and contained clean fluid; the other (13) was used only to collect the contaminated fluid while water was injected into the system. This arrangement prevented reentrainment of water droplets into the test section.

Droplet Size Measurement Techniques

Droplet Encapsulation. With this method it is possible to prevent droplet coalescence and preserve the size distribution, in a properly taken sample, as follows. A protective coating is formed quite fast on the surface of each droplet, when a small quantity of a certain monomer, present in the dispersed phase, comes in contact with another monomer dissolved in the continuous phase. Recently, Mlynek and Resnick (1972) successfully employed this technique to measure drop size distributions in an agitated vessel. The reacting compounds in their experiments were 0.05% wt piperazine in the aqueous, continuous phase and 0.05% wt terephthalic acid chloride in the dispersed phase, which was a mixture of carbon tetrachloride and iso-octane. The same additives were used in our study. A concentration 0.75% wt anhydrous piperazine dissolved in deionized water gave the best results. Indigo-caramine dye was added to the water to obtain a deep blue color before injection into the line. Two different liquids, that is, kerosene and viscous transformer oil, were used as the continuous phase.

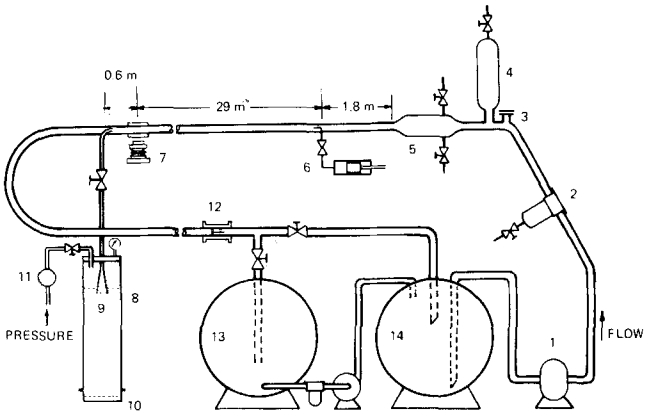

Fig. 1. Schematic of flow system.

A sampling vessel (No. 8, Figure 1) was made out of a transparent acrylic pipe section, ~1.15 m long, with an inside diameter of 13.9 cm. This vessel was equipped with a gauge and a regulator (11) in order to adjust the pressure and withdraw fluid from the pipe under nearly isokinetic conditions. It was filled up to about 70% of its capacity with kerosene containing 0.2% wt dissolved terephthaloyl chloride. This compound was first dissolved in 300 to 400 cm^3 of carbon tetrachloride and then mixed with an appropriate amount of kerosene. The short sampling tube had a conical end (9), immersed approximately 2 cm into the fluid, in order to reduce the discharge velocity of the droplets into the vessel, thus increasing their settling time. Upon contact of the droplets with the sampler fluid, the piperazine dissolved in the water reacted with the terephthaloyl chloride forming a protective coating.

The bottom of the vessel was covered with a layer of viscous silicone oil (Dow Corning 200, 1000 centistokes) approximately 7 mm thick. The function of this layer was twofold: to terminate the reaction between droplets and the continuous phase which, beyond a certain time, tends to produce rough coatings on the droplet surfaces and to result, occasionally, in agglomerates; to prevent water wetting of, and droplet sticking onto, the bottom plate and to preserve the spherical shape of the settled drops. The density of the silicone oil was between that of kerosene and water. The bottom of the vessel on which droplets deposited was made of optical quality, thick glass plate. As indicated in Figure 1, the lower section of the sampling vessel (10) could be disengaged by using a Victaulic connector. This short section was transferred to a stand without disturbing the already settled drops, and pictures were taken from the bottom.

This technique was in general very satisfactory. Sampling over a period of 3 to 5 s provided a sufficiently large number of droplets which were distributed on the bottom plate without excessive crowding and overlapping. Pictures with total magnification five to twenty-three times the real object were used to measure droplet size distributions under various pipeline flow conditions. Usually all the droplets in a picture were measured with an accurate ruler under additional magnification. In most cases more than one picture was used to obtain a total count of more than 300 drops.

Photographic Technique. During the tests with kerosene, photographs of the dispersions were taken, concurrently with the droplet encapsulation data, in order to compare the two techniques. A test section very similar to that used by Collins (1967) was located approximately 0.8 m upstream of the sampling tube. Two diametrically opposite holes were drilled with their centers on the vertical axis of the pipe. Optical quality glass disks were mounted essentially flush with the pipe surface and held in place by a Plexiglas collar.

The camera was focused at a distance of 6.4 mm from the inner pipe surface. The viewing ports and camera were aligned on an axis approximately 15 deg from the vertical pipe diameter. A General Radio Strobotac, type 153-AB light source was located diametrically opposite to the camera, 23 cm from the pipe. The flash duration was ~0.5 μs. A Nikon F camera was used with 1.4 Nikon lens and a specially made 43 cm extension between camera body and lens to obtain the desired magnifica-

Table 1. Experimental Conditions

Run number	Mean velocity, m/s	Temperature, °C	Density, ρ_c g/cm³	Viscosity, μ_c mN s/m²	Water injection rate, cm³/s	Continuous Phase
1	1.52	22.2	0.798	1.82	6.0	Kerosene
2	1.52	22.2	0.798	1.82	6.0	
3	2.98	22.2	0.798	1.82	11.9	
4	1.18	22.5	0.798	1.81	4.7	
5	2.57	21.1	0.799	1.86	10.3	
6	2.22	23.3	0.797	1.77	8.9	
7	1.84	21.9	0.798	1.83	7.5	
11	3.00	20.6	0.892	16.00	11.8	Transformer oil
12	1.19	21.4	0.892	15.42	6.3	
14	1.52	17.5	0.894	18.27	6.1	
15	1.86	18.6	0.893	17.43	6.1	
16	2.24	21.4	0.892	15.42	8.9	
17	2.60	26.1	0.888	12.47	10.3	
18	2.08	23.3	0.890	14.12	8.4	

tion. The camera setting was F-4 at 1/30 with FX synchronization. Panatomic X film was used and developed in HC-110 mixture B. The negatives were enlarged six times and prints were made on Polycontrast F paper.

The same type of camera and film were used to photograph the samples of encapsulated droplets. Nikon bellows and a Nikon F-2 lens were employed. A camera setting of F-4 gave the best depth of field and sharpness in this case. In order to light the sample tray, a photo-flood was mounted 0.6 m above the sample. The light was filtered through a sheet of diffusion paper located 30 cm above the sample.

Experimental Conditions

Experiments were carried out with kerosene (Dispersol by Shell Oil Company) and a more viscous transformer oil (Texaco Transformer Oil No. 55) as continuous phases. The dispersed phase was deionized water with the additive required for droplet encapsulation. Interfacial tension measurements with a DuNouy tensiometer gave the following results:

Kerosene/water	σ = 33.1 mN/m at 22.8°C 31.7 mN/m at 24.4°C
Trans. oil/water	σ = 35.0 mN/m at 17.8°C 33.7 mN/m at 23.3°C 32.7 mN/m at 26.7°C

Experimental conditions are summarized in Table 1. Mean velocities varied between ~1.2 and 3.0 m/s. After a pipeline flow rate was selected, the water injection system was adjusted to provide a steady injection rate of 0.20% by volume. Only in runs No. 12 and 15 the water volume concentration was 0.26% and 0.16%, respectively.

Samples and line photographs were taken simultaneously. The raw data obtained from direct droplet size measurements were digitized and processed in the computer. In order to obtain size distributions and $\overline{d}_{32}$, size intervals of 100 μm (up to 1000 μm) and 200 μm (above 1000 μm) were selected.

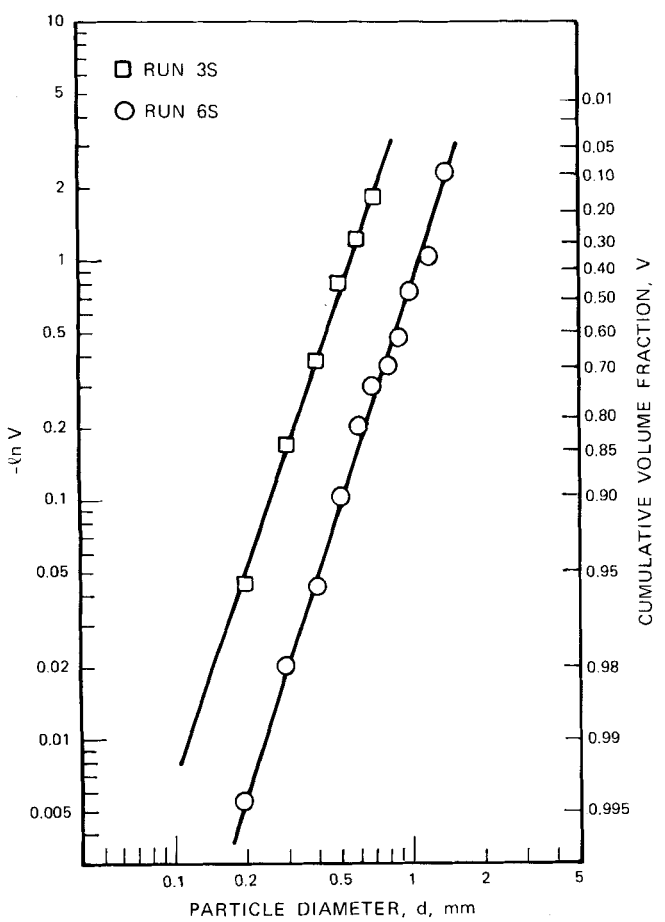

Fig. 2. Drop size distribution of water in kerosene, represented by a Rosin-Kammler type of function. $\overline{U}$ = 2.98 and 2.22 m/s.

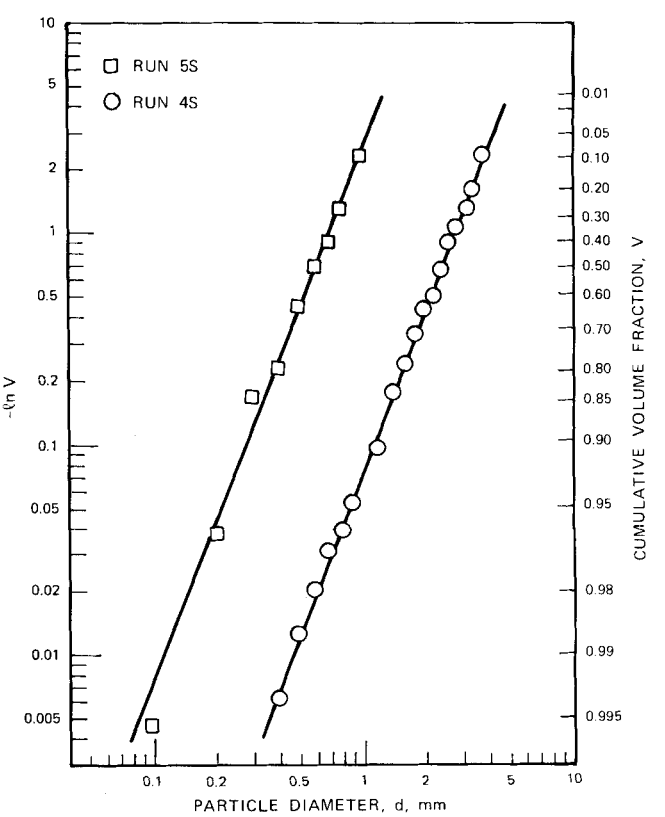

Fig. 3. Drop size distribution of water in kerosene, represented by a Rosin-Rammler type of function. $\overline{U}$ = 2.57 and 1.18 m/s.

RESULTS

Figures 2 and 3 show data obtained from samples of water dispersed in kerosene at various velocities. The linearity of these data, plotted in logarithmic coordinates, suggests that the Rosin-Rammler (1933) equation

$$V = \exp\left[-\left(\frac{d}{d^*}\right)^n\right] \tag{8}$$

provides a very satisfactory representation of the measured distributions, especially at the large diameter end of the spectra. In Equation (8), V is the cumulative volume fraction of particles with diameters greater than d, and the parameters n and d^* are the slope of the line and the diameter corresponding to $V = 0.3679$, respectively. Alternatively, one can use the fraction V corresponding to any other characteristic diameter to specify the distribution. If d_{95} is used, Equation (8) becomes

$$V = \exp\left[-2.996\left(\frac{d}{d_{95}}\right)^n\right] \tag{9}$$

An equally good, and in many cases better, fit of the data presented here is obtained by the upper limit log-probability function, suggested by Mugele and Evans (1951). The volume distribution function in this case is given as

$$\frac{d(1-V)}{dz} = \frac{\delta}{\sqrt{\pi}}\exp(-\delta^2 z^2) \tag{10}$$

and upon integration

$$V = \frac{1}{\sqrt{\pi}}\int_{\delta z}^{\infty}\exp(-x^2)dx = \frac{1}{2}[1 - \operatorname{erf}(\delta z)] \tag{11}$$

where

$$z = \ln\left[\frac{ad}{d_{\max} - d}\right] \tag{12}$$

and

$$a = \frac{d_{\max} - d_{50}}{d_{50}} \tag{13}$$

Three parameters are required to specify this distribution, that is, $d_{\max}$, a, and δ, and can be obtained from the data as

$$\frac{d_{\max}}{d_{50}} = \frac{d_{50}(d_{90} + d_{10}) - 2d_{90}d_{10}}{d_{50}^2 - d_{90}d_{10}} \tag{14}$$

and

$$\delta = \frac{0.394}{\log_{10}\left[\frac{v_{90}}{v_{50}}\right]} \tag{15}$$

where $v_i = d_i/(d_{\max} - d_i)$. Given the three parameters, the Sauter mean diameter $\overline{d}_{32}$, and d_{95} are calculated as

$$\overline{d}_{32} = \frac{d_{\max}}{1 + a \cdot \exp\left[\frac{1}{4\delta^2}\right]} \tag{16}$$

and

$$d_{95} = \frac{\frac{d_{\max}}{a}\exp\left[\frac{1.163}{\delta}\right]}{1 + \frac{1}{a}\exp\left[\frac{1.163}{\delta}\right]} \tag{17}$$

The data shown in Figures 2 and 3 have been replotted in log-probability coordinates in Figures 4 and 5, respectively. It is evident that the upper limit log-probability function provides a very satisfactory representation of the data. Drop size distribution parameters for all the runs made with water-in-kerosene dispersions are summarized in Table 2. This table also includes $\overline{d}_{32}$, calculated directly from the raw data, as well as the diameter of the largest drop in a sample.

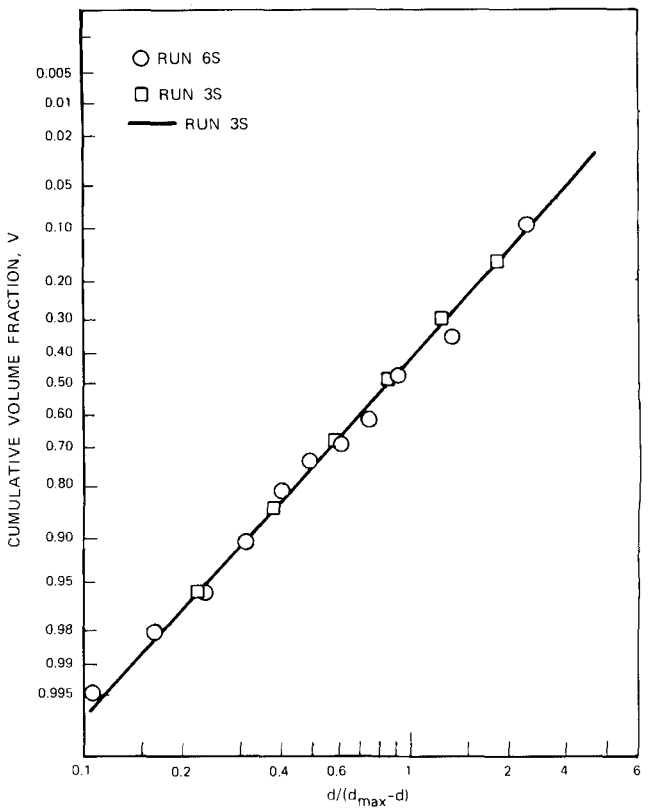

Fig. 4. Drop size distribution of water in kerosene, represented by an upper limit log-probability function. $\overline{U} = 2.98$ and 2.22 m/s.

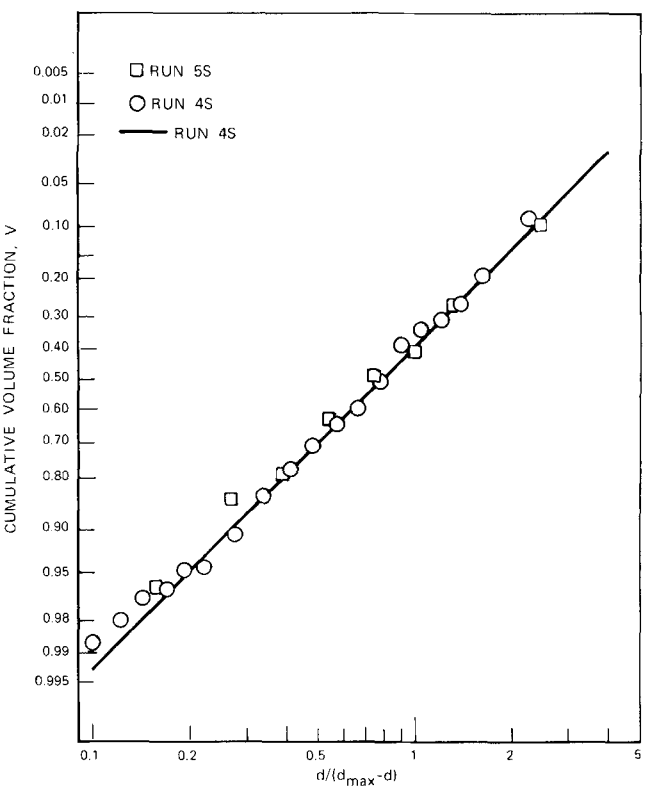

Fig. 5. Drop size distribution of water in kerosene, represented by an upper limit log-probability function. $\overline{U} = 2.57$ and 1.18 m/s.

Table 2. Drop Size Distribution Parameters from Data with Low Viscosity Continuous Phase (Kerosene). Data Obtained from Samples

Run number	Velocity $\overline{U}$, m/s	Upper limit log-normal distribution a	δ	d_{max}, μm	d_{95}, μm	$\overline{d}_{32}$, μm	Rosin-Rammler distribution n	d_{95}, μm	Data $\overline{d}_{32}$, μm	d_{max}†, μm
3S	2.98	1.174	0.915	1 074	808	416	2.90	820	407	756
5S	2.57	1.339	0.827	1 404	1 057	479	2.53	1 075	455	1 111
6S	2.22	1.163	0.965	2 087	1 547	828	3.07	1 550	794	1 547
7S	1.84	1.535	0.809	3 600	2 638	1 108	2.31	2 650	1 066	2 603
1S*	1.52	0.938	0.953	4 767	3 733	2 133	3.30	3 800	2 083	4 242
2S	1.52	1.495	0.881	5 338	3 814	1 743	2.52	3 850	1 887	4 310
4S	1.18	1.269	0.845	5 491	4 158	1 960	2.58	4 250	1 942	5 172
Arithmetic average		1.329	0.874				2.65			

* Excluded from averaging.
† Diameter of largest measured drop.

A number of interesting observations can be made, based on the results of Table 2. The characteristic diameters d_{95} obtained by fitting the data with an upper limit log-probability function are at most 2% smaller than d_{95} obtained with the Rosin-Rammler equation. This close agreement is due to the fact that in the range $V \simeq 0.05$ to 0.95 the deviation of the Rosin-Rammler from the log-probability distribution is small and comparable to the standard deviation of the data points. The simple Rosin-Rammler equation, with only two parameters, is obviously more convenient for engineering calculations. It should be stressed, however, that the upper limit log-probability function is more accurate at both ends of the size spectrum. In particular, the parameter d_{max} has an obvious physical significance, and it is very appropriate for the description of processes and/or data characterized by a maximum stable size. Other advantages of the upper limit log-probability function are discussed in detail by Mugele and Evans (1951).

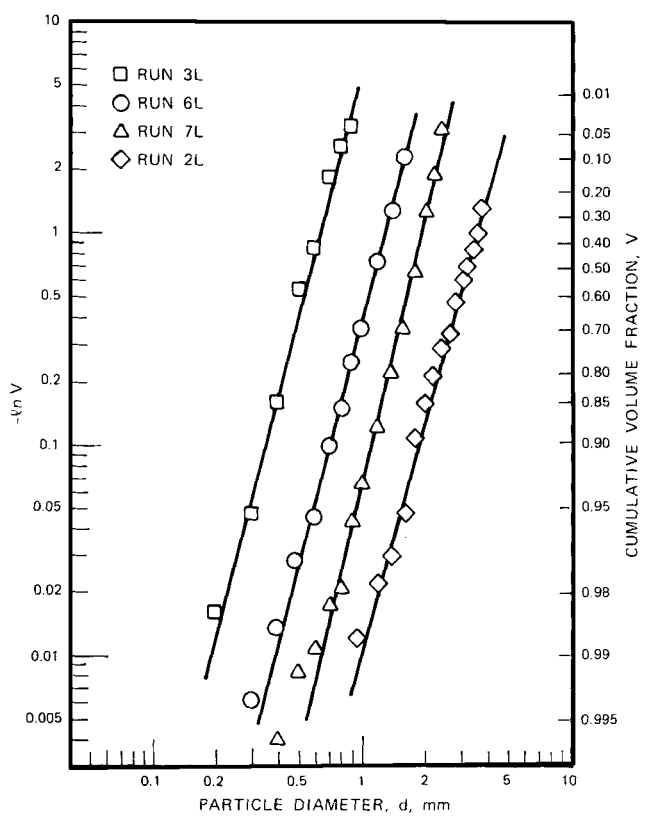

Fig. 6. Drop size distribution of water in kerosene, obtained from line photographs.

Table 3. Comparison Between Data from Samples and Photographs of Flowing Dispersions. Continuous Phase: Kerosene

Run number	Velocity $\overline{U}$, m/s	Samples n	Samples d_{95}, μm	Line photographs n	Line photographs d_{95}, μm
3	2.98	2.90	820	3.88	830
5	2.57	2.53	1 075	4.03	1 100
6	2.22	3.07	1 550	3.86	1 700
7	1.84	2.31	2 650	4.25	2 450
2	1.52	2.52	3 850	3.64	4 700
4	1.18	2.58	4 250	4.27	6 250
Arithmetic average		2.65		3.99	

The good agreement, shown in Table 2, between $\overline{d}_{32}$ computed directly from the data and from Equation (11) is also a measure of success of the log-probability function. However, the diameters of the largest measured drops are closer to d_{95} than to d_{max} obtained from Equation (11). This can be explained as follows. Assuming that the upper limit log-probability equation describes precisely drop distributions, the probability of having a particle of size d approaching d_{max} is infinitely small. Moreover, for most of the distributions measured in this study, the upper 5% by volume, associated with d_{95}, corresponds to a number percentage of only ~0.5. In our experiments, the total number of drops in a sample was 250 to 500. Therefore, in a sample representative of the true distribution, the largest one to two drops should have diameters close to d_{95}.

One of the most interesting results emerging from the data of Table 2 is that the parameters a, δ, and n, perhaps with the exception of run 1, are fairly constant and show no influence of the flow rate on the shape of the distribution. Obviously, this result is of significance at least from the viewpoint of correlating the data.

The above data were obtained with the special droplet encapsulation technique. Figure 6 shows drop size distributions obtained from photographs of flowing water-in-kerosene dispersion, at mean velocities $\overline{U} = 1.52$ to 2.98 m/s. These distributions are self-consistent and can be satisfactorily described by the Rosin-Rammler and the upper limit log-probability functions as in the previous case. The Rosin-Rammler parameters for data obtained, under the same conditions, with the two different techniques are listed in Table 3. The drop diameters d_{95} are in good agreement, except at the two smallest flow rates. The slope n is fairly constant and apparently independent of flow rate in each case, but quite large in the case of line photographs ($n \simeq 4$). Obviously, the mean diameters

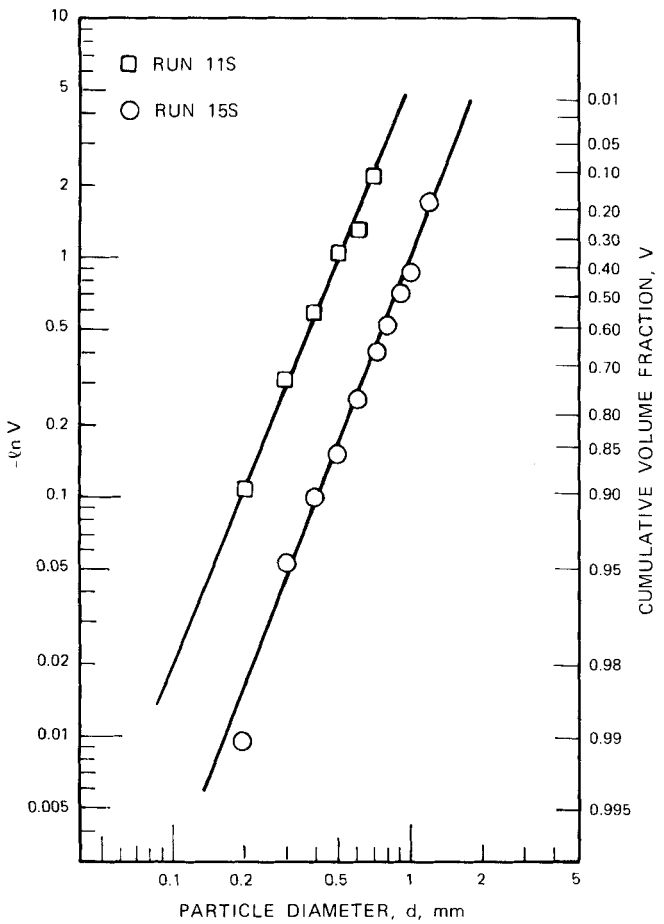

Fig. 7. Drop size distribution of water in transformer oil, represented by a Rosin-Rammler type function. $\overline{U} = 3.00$ and 1.86 m/s.

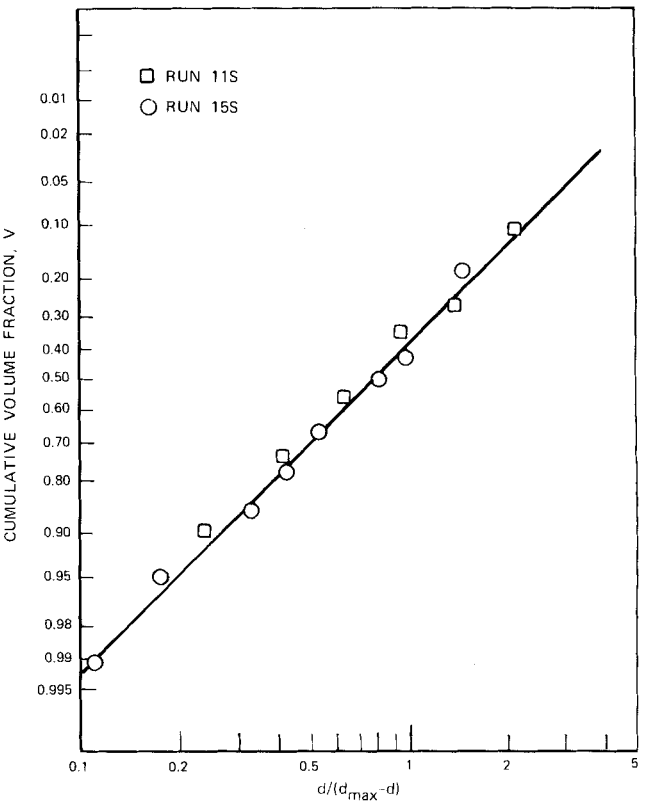

Fig. 8. Drop size distribution of water in transformer oil, represented by an upper limit log-probability function. $\overline{U} = 3.00$ and 1.86 m/s.

obtained from line photographs are considerably greater than those measured from the samples.

This discrepancy is very likely due to the following drawbacks of the photographic technique:

1. The camera was focused in a region of the pipe cross section, close to the bottom, where the local time-average drop size distributions may have been coarser than the overall average, due to the effect of gravity (Karabelas, 1977).

2. The quality of most pictures obtained from the line was not satisfactory, perhaps due to the relatively small depth of field. The sharpness of the drops in each print varied between well focused, sharp particles, and obscure images requiring a subjective judgment to decide which drops should be measured. As was also pointed out by Collins (1967), such poor picture quality may have biased the distributions toward the larger drops.

3. The instantaneous velocity of a drop is expected to increase with decreasing size. Therefore, for a fixed flash duration, a relatively higher percentage of small drops may appear to be out of focus even if they are within the photographed depth of field.

The above possible sources of error (especially the last two) were absent in the case of still photographs of samples withdrawn from the pipeline. Furthermore, we observed a very large number of small drops (below ~200 μm) in the discharge tank (13, Figure 1), which did not appear to be represented in the spectra obtained from line photographs. For these reasons, the encapsulation technique was judged more reliable and the data obtained from samples much more representative of the true distributions. Therefore, in subsequent experiments with the more viscous transformer oil as the continuous phase, only data from samples were collected systematically.

Figure 7 shows drop size spectra of water in transformer

Table 4. Drop Size Distribution Parameters from Data with Viscous Continuous Phase (Transformer Oil). Data Obtained from Samples

Run number	Velocity $\overline{U}$, m/s	Upper limit log-normal distribution a	δ	d_{max}, μm	d_{95}, μm	$\overline{d}_{32}$, μm	Data $\overline{d}_{32}$, μm	d_{max}†, μm	Rosin-Rammler distribution n	d_{95}, μm
11S	3.00	1.369	0.818	1 030	775	345	347	730	2.42	790
17S	2.60	1.286	0.888	1 097	814	397	401	951	2.73	825
10S	2.24	1.231	0.914	1 383	1 028	520	512	1 110	2.82	1 045
18S	2.08	1.819	0.792	1 579	1 113	426	428	1 217	2.13	1 130
15S	1.86	1.283	0.839	2 009	1 521	710	700	1 381	2.54	1 540
14S	1.52	1.230	0.858	2 498	1 896	916	840	1 805	2.63	1 935
12S	1.19	1.573	0.828	2 625	1 894	804	844	1 987	2.34	1 925
Arithmetic average		1.399*	0.848						2.51	

* Average $a = 1.329$ if run 18 is excluded.
† Diameter of largest measured drop.

oil, at mean velocities $U = 3.00$ and 1.86 m/s. The same data have been replotted in log-probability coordinates in Figure 8. As in the case of water/kerosene dispersions, both the Rosin-Rammler and the upper limit log-probability functions give a very good fit of the data. The distribution parameters for all the runs with transformer oil are listed in Table 4.

These distributions display exactly the same characteristics as those of the water/kerosene system. The diameters d_{95} obtained basis the Rosin-Rammler and log-probability equations are almost identical; the largest measured droplets are closer to d_{95} than to the parameters d_{max}; the Sauter mean $\overline{d_{32}}$ directly computed from the data are in good agreement with those obtained from Equation (11), and the parameters a, δ, and n appear again to be independent of flow rate. Furthermore, the mean values of these parameters are nearly equal to those obtained with water-in-kerosene dispersions. A direct consequence of this important observation is that if a, δ, and n are nearly constant over a range of conditions, one needs only a reliable estimate of d_{max} or d_{95} in order to predict the entire distribution.

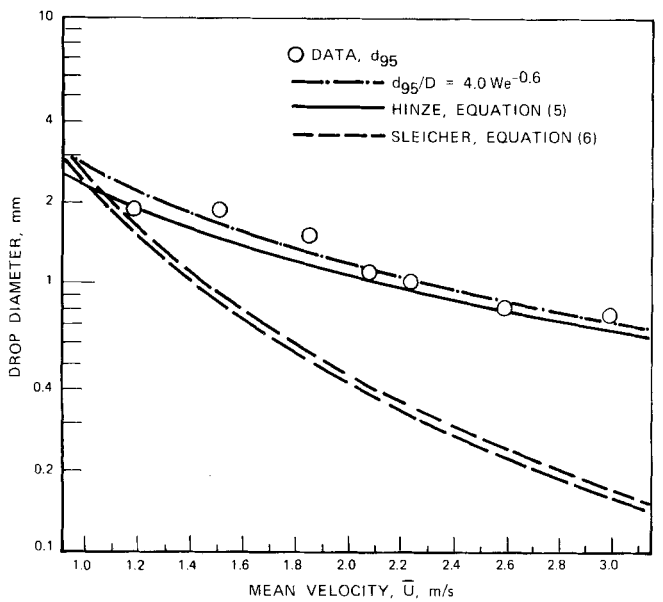

Fig. 9. Effect of velocity on maximum drop diameter. Water dispersed in transformer oil (ν_c = 14.2 to 20.5 mm²/s).

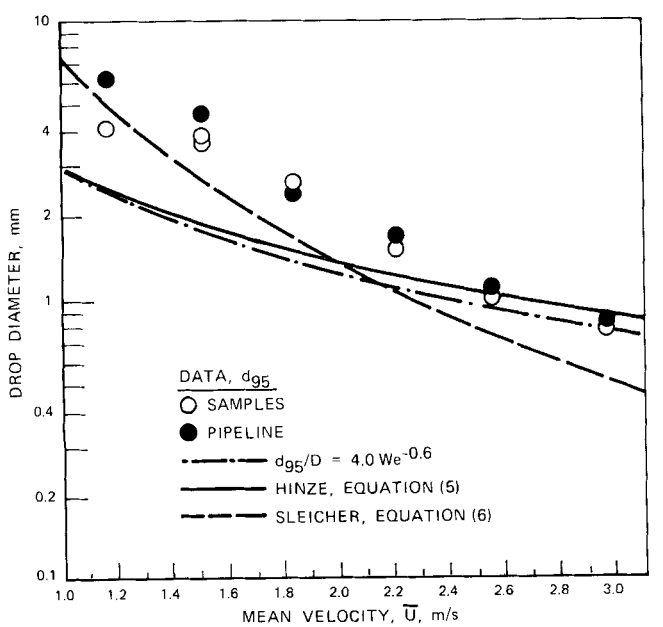

Fig. 10. Effect of velocity on maximum drop diameter. Water dispersed in kerosene (ν_c = 2.2 to 2.3 mm²/s).

CORRELATION OF MAXIMUM DROP SIZE DATA

In Figures 9 and 10, the data on d_{95} are compared with the Sleicher correlation and the Hinze model predictions. The data obtained with transformer oil are in good agreement with Equation (5), whereas predictions of d_{95} based on the Sleicher correlation are five times smaller at high velocities. The disagreement of this correlation with data on d_{max}, for which it was originally developed, is even greater. Furthermore, the data of Figure 9 show an almost linear dependence of d_{95} on velocity that is far from the $\bar{U}^{-2.5}$ dependence suggested by Sleicher.

The data of Figure 10, obtained with kerosene as the continuous phase, at first look appear to agree somewhat better with the Sleicher than with the Hinze correlation. However, after careful examination of the conditions under which these data were obtained, we concluded that the effect of gravity is responsible for the deviation of measured d_{95} from Equation (5), at velocities smaller than 2.4 m/s. As shown elsewhere (Karabelas, 1977), if the carrier liquid viscosity is small, the largest droplets tend to concentrate at the bottom of a horizontal pipe at low velocities. This tendency may have affected our data as follows:

1. Since the sampling tube was located below the pipe center line, the samples became less representative of the average distribution with decreasing flow rate. The consistently greater deviation of d_{95} from the predictions of Equation (5) with decreasing flow rate, shown in Figure 10, is indicative of this effect.
2. The increasing mean concentration at the pipe bottom, with decreasing flow rate, coupled with a possible velocity lag of the largest droplets, may have promoted coalescence and formation of drops somewhat larger than those encountered in dilute, homogeneous dispersions.

At this point we must conclude that the Hinze/Kolmogorov model is more reliable than the Sleicher correlation because it has a more solid theoretical basis and it is generally in better agreement than Equation (6) with the data presented here. Next, we shall briefly review the conditions under which this model [Equation (2)] applies to pipe flow. In particular, we shall examine whether the mean rate of energy dissipation $\bar{\epsilon}$, substituted into Equation (2), provides satisfactory estimates of d_{max} or d_{95}.

The main assumption involved in the development of Equation (2) is that the flow is homogeneous and isotropic. In such a case, most of the kinetic energy of turbulent fluctuations is contained in the range of wave numbers (inertial subrange) where the Kolmogorov distribution law is valid. As is well known (see, for example, Tennekes and Lumley, 1972), the same law describes energy distribution in the inertial sublayer of pipe flow, that is, at y^+ greater than 30 to 35 where Equation (2) is expected to be valid. If the Blasius Equation (4) is employed to estimate u_*, $y^+ = 35$ corresponds to a distance from the wall

$$\frac{y}{R} \simeq \frac{352}{Re^{7/8}} \qquad (18)$$

where R is the pipe radius. Figure 11 shows that, for a given pipe diameter, the thickness of the buffer layer is greatly reduced at high Reynolds numbers; that is, the lower boundary of the inertial sublayer is very close to the wall. For example, in a 25.4 cm ID pipe at $Re = 10^6$, the inertial sublayer ($y^+ \simeq 35$) is within 250 μ from the pipe wall.

Using Equation (5) one can show that, in almost all cases of practical interest, the maximum stable droplet sizes generated in the turbulent core are larger than the wall layer thickness corresponding to $y^+ = 35$. Moreover, it is very likely that these relatively large droplets will have a tendency to migrate away from the wall owing to lateral forces similar to those observed in laminar pipe flow (Segré and Silberberg, 1962). It appears therefore, that breakup of the largest droplets will take place primarily inside the inertial sublayer.

The local rate of energy dissipation per unit mass ϵ_l in the inertial sublayer is inversely proportional to the distance from the wall; that is

$$\epsilon_l \simeq \frac{u_*^3}{ky} \tag{19}$$

if we assume (for example, Tennekes and Lumley, 1972) a balance of turbulence energy production by viscous dissipation. The von Karman constant k is approximately 0.4. It can easily be shown that the distance from the wall at which the local rate of dissipation ϵ_l is equal to the mean $\bar{\epsilon}$ [Equation (3)] is given by

$$\left.\frac{y}{R}\right|_{\epsilon_l=\bar{\epsilon}} \simeq \frac{0.2486}{Re^{1/8}} \tag{20}$$

This function has been plotted in Figure 11.

It is evident now that the use of the mean rate $\bar{\epsilon}$ in Equation (2) would give conservative estimates of d_{max} or d_{95} at high flow rates. Indeed, for usual liquids at high Reynolds numbers, the largest droplets, of relative size $\sim d_{max}/D$, that can survive at a distance from the wall $y/R|_{\bar{\epsilon}}$ may be comparable in size or larger than the thickness of the buffer layer, but they are small compared to $y/R|_{\bar{\epsilon}}$. These droplets can move deeper into the inertial sublayer, that is, closer to the wall, where the local energy dissipation rate ϵ_l is larger than $\bar{\epsilon}$. Further breakup will, therefore, result in d_{max} smaller than that corresponding to $\bar{\epsilon}$.

Using the local dissipation rate ϵ_l and the value of $C = 0.725$, suggested by Hinze, into Equation (2) we obtain

$$\frac{d_{95}}{D} = 2.645\left[\frac{\sigma}{D\rho_c\bar{U}^2}\right]^{0.6} Re^{0.15}\left[\frac{y}{R}\right]^{0.4} \tag{21}$$

Following the previous arguments, it is reasonable to assume that there is a characteristic distance from the wall $y/R|_c$ associated with the largest stable droplets. At high Re, this distance is likely to be between $y^+ \simeq 35$ and the distance corresponding to $\epsilon_l = \bar{\epsilon}$.

At present, it is very difficult to provide a more accurate definition of $y/R|_c$, on physical grounds, although one could develop speculative theories relating $y/R|_c$ to the kinematics of large droplets near the wall and their mean residence time relative to the characteristic time required for breakup. In order to simplify Equation (21) and provide a correlation more accurate than (5), we have selected the following expression:

$$\left.\frac{y}{R}\right|_c = \frac{2.8}{Re^{3/8}} \tag{22}$$

As shown in Figure 11, the slope of this line is the mean difference of the slopes of the lines $y^+ = 35$ and $\epsilon_l = \bar{\epsilon}$ and essentially eliminates the Re dependence from Equation (21). The constant in Equation (22) has been obtained by assuming that the lines $y/R|_c$, $\epsilon_l = \bar{\epsilon}$ and $y^+ = 35$ have a common point of intersection.

Substituting Equation (22) into (21), we obtain

$$\frac{d_{95}}{D} = 4.0\,We^{-0.6} \tag{23}$$

where $We = D\rho_c\bar{U}^2/\sigma$ is a dimensionless Weber number based on pipe diameter and mean velocity. As shown in Figures 9 and 10, this equation fits our data somewhat better than Equation (5). It is also expected that Equation (23) provides reliable estimates of d_{95} throughout the Re range of practical interest. However, it should be used with caution in the case of a very viscous dispersed phase in which breakup may be influenced by inertial as well as viscous forces.

DISCUSSION

For measurements of size distribution, the droplet encapsulation technique appears to be more accurate than the photographic method also employed in this as well as in previous studies. All the data obtained with the former technique are self-consistent and provide useful information about the effect of flow rate on the size spectrum. Of particular interest is the similarity of the measured spectra, which permits their representation by a single well-known distribution function such as the upper limit log-probability or the Rosin-Rammler equation.

Collins (1967) and Collins and Knudsen (1970) reached different conclusions by interpreting size distribution data obtained with a photographic technique. This led to reevaluation of some of Collins' data and comparison with our results (see Appendix). We concluded that most of Collins' data, plotted in terms of cumulative volume fractions, can indeed be fitted with a Rosin-Rammler or

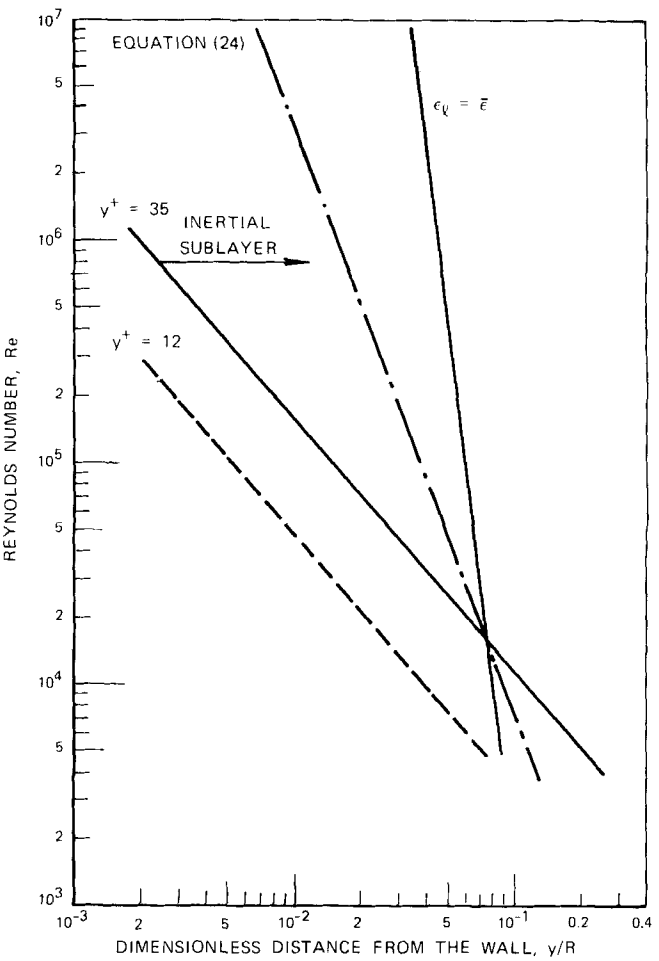

Fig. 11. Effect of Reynolds number on wall layer thickness and on locus of $\epsilon_{local} = \bar{\epsilon}$.

an upper limit log-probability type of distribution function, as is the case with our data. However, the characteristic slope of these distributions seems to be high ($n \simeq 4.0$) and probably unrepresentative of the true size spectra. This is attributed to inaccuracies inherent in the photographic technique. Data on d_{95} obtained from the above distributions are in better agreement with the correlation proposed here [Equation (23)] than with Sleicher's correlation. Finally, Collins' data indicate that the test section length used in his as well as in our study (~576 and 600 pipe diameters, respectively) is sufficient to form the maximum stable drop diameter.

At present, the development of a rigorous theory to predict equilibrium size spectra in pipe flow appears to be a very difficult task. The mathematical framework suggested by Valentas et al. (1966) is certainly useful in this respect. However, a great deal of information regarding basic fluid mechanical aspects of the problem (mainly, particle kinematics in a turbulent shear field) is required before real progress can be made. The data presented in this paper are generally considered encouraging in that they reveal some basic characteristics of drop size spectra. Additional data, under conditions different than those of our study, are of course required to firm up the conclusions reached here and to guide future modeling studies.

ACKNOWLEDGMENT

The author is grateful to Shell Development Company for permission to publish this paper.

NOTATION

a = parameter in upper limit log-probability distribution function, Equation (13), dimensionless
C' = proportionality constant
D = pipe inside diameter, L
d = particle diameter, μ, L
$\overline{d}_{32}$ = Sauter mean diameter; volume to area mean diameter, L
d_{max} = maximum stable drop diameter; also parameter in upper limit log-probability Equation (11), L
d_{50}, d_{95} = particle diameter corresponding to 50 and 95% vol, respectively, of particles smaller than d_{50} and d_{95}, L
d_i' = designates characteristic drop diameters based on cumulative number fractions, L
d^* = drop diameter corresponding to $V = 0.3679$, L
f = friction factor; $\dfrac{\Delta P}{\Delta L}\dfrac{D}{2\rho_c \overline{U}^2}$, dimensionless
R = pipe inside radius, L
Re = Reynolds number, $D\overline{U}\rho_c/\mu_c$, dimensionless
$\overline{U}$ = mean flow velocity, LT^{-1}
u = local fluctuating velocity, LT^{-1}
u_* = friction velocity, $\left[\dfrac{\Delta P}{\Delta L}\dfrac{D}{4\rho_c}\right]^{1/2}$, LT^{-1}
V = cumulative volume fraction, dimensionless
We = Weber number, $\rho_c D\overline{U}^2/\sigma$, dimensionless
y^+ = dimensionless distance from pipe wall, $u_* y/\nu$

Greek Letters

$\Delta P/\Delta L$ = pressure drop, $ML^{-2}T^{-2}$
δ = parameter in upper limit log-probability, Equation (10), dimensionless
ϵ = energy dissipation per unit mass and time, L^2T^{-3}
ϵ_l = local rate of energy dissipation per unit mass, L^2T^{-3}
$\overline{\epsilon}$ = mean rate of energy dissipation per unit mass; in pipe flow $\overline{\epsilon} = 2f\overline{U}^3/D$, L^2T^{-3}
μ_c, μ_d = dynamic viscosity of continuous and dispersed liquid phase, respectively, $ML^{-1}T^{-1}$
ν = kinematic viscosity, μ/ρ, L^2T^{-1}
ρ_c, ρ_d = density of continuous and dispersed liquid phase, respectively, ML^{-3}
σ = interfacial tension, MT^{-2}

LITERATURE CITED

Clay, P. H., "The Mechanism of Emulsion Formation in Turbulent Flow," Akademie van Wetenschappen (Amsterdam), *Proceedings*, **43**, 852-965 (1940).

Collins, S. B., "Drop Size Distribution Produced by Turbulent Pipe Flow of Immiscible Liquids," Ph.D. thesis, Ore. State University, Corvallis (1967).

———, and J. G. Knudsen, "Drop Size Distributions Produced by Turbulent Pipe Flow of Immiscible Liquids," *AIChE J.*, **16**, No. 6, 1072-1080 (Nov., 1970).

Hinze, J. O., "Fundamentals of the Hydrodynamic Mechanism of Splitting in Dispersion Processes," *ibid.*, **1**, No. 3, 289-295 (1955).

Karabelas, A. J., "Vertical Distribution of Dilute Suspensions in Turbulent Pipe Flow," *ibid.*, **23**, No. 4, 426-434 (1977).

Kolmogorov, A. N., "On the Breaking of Drops in Turbulent Flow," *Doklady Akad. Nauk. U.S.S.R.*, **66**, 825 (1949).

Kubie, J, and G. C. Gardner, "Drop Sizes and Drop Dispersion in Straight Horizontal Tubes and in Helical Coils," *Chem. Eng. Sci.*, **32**, No. 2, 195-202 (1977).

Levich, V. G., *Physicochemical Hydrodynamics*, Translated from the Russian by Scipta Technica, Inc., Prentice Hall, Inc., Englewood Cliffs, N.J. (1962).

Mlynek, Y., and W. Resnick, "Drop Sizes in Agitated Liquid-Liquid Systems," *AIChE J.*, **18**, No. 1, 122-127 (Jan., 1972).

Mugele, R. A., and H. D. Evans, "Droplet Size Distribution in Sprays," *Ind. Eng. Chem.*, **43**, No. 6, 1317-1324 (June 1951).

Paul, H. I., and C. A. Sleicher, Jr., "The Maximum Stable Drop Size in Turbulent Flow: Effect of Pipe Diameter," *Chem. Eng. Sci.*, **20**, 57-59 (1965).

Rosin, P., and E. Rammler, "The Laws Governing the Fineness of Powdered Coal," *J. Inst. Fuel*, **7**, 29-36 (Oct., 1933).

Segré, G., and A. Silberberg, "Behaviour of Macroscopic Rigid Spheres in Poiseuille Flow. Part 2," *J. Fluid Mech.*, **14**, 136-157 (1962).

Shinnar, R., "On the Behavior of Liquid Dispersions," *J. Fluid Mech.*, **10**, 259 (1961).

Sleicher, C. A., Jr., "Maximum Stable Drop Size in Turbulent Flow," *AIChE J.*, **8**, No. 4, 471-477 (1962).

Sprow, F. B., "Distribution of Drop Sizes Produced in Turbulent Liquid-Liquid Dispersions," *Chem. Eng. Sci.*, **22**, 435 (1967).

Tennekes, H., and J. L. Lumley, *A First Course in Turbulence*, The MIT Press, Cambridge, Mass. (1972).

Valentas, K. J., et al., "Analysis of Breakage in Dispersed Phase Systems," *Ind. Eng. Chem. Fundamentals*, **5**, No. 2, 271-279 (1966).

APPENDIX: COMPARISON OF DATA BY COLLINS WITH THE RESULTS OF THIS STUDY

The data obtained by Collins (1967) will be briefly reexamined in the light of the results obtained in this study. The most complete set of data was taken with 1.3% light hydrocarbon (Shellsolv) dispersed in water. Although not clearly stated in Collins' thesis, all the data are presented in terms of cumulative number fractions instead of the more conventional cumulative volume fractions. For the types of distributions measured by Collins, it can be easily shown that only 0.5 and 9% of the droplet population corresponds, respectively, to ~5 and ~50% of the dispersed phase volume, that is, $d'_{99.5} \simeq d_{95}$ and $d'_{91} \simeq d_{50}$.

Table 5 shows data on the variation of $d'_{99.5}$ and d'_{91} with axial distance which were obtained from distributions measured at three different points in the pipe cross sections, that is, $y/R \simeq 0.05$, 0.10, and 0.40. The data suggest that at 576 pipe diameters downstream of the injection point, the largest stable droplets were already formed. The scatter in these data, and especially in $d'_{99.5}$, does not permit further analysis. It will be

Table 5. Effect of Axial Distance from Injection Point x/D on Characteristic Drop Sizes, Obtained from Collins' Data (1967, pp. 56, 70, and 71) 1.3% Shellsolv Dispersed in Water at 4.88 m/s

	$y/R = 0.05$		$y/R = 0.10$		$y/R = 0.40$	
x/D	$d'_{99.5}$, μm	d'_{91}, μm	$d'_{99.5}$, μm	d'_{91}, μm	$d'_{99.5}$, μm	d'_{91}, μm
27	610	325	640	320	590	320
209	415	280	460	285	430	300
421	415	270	390	285	380	300
576	360	280	380	265	400	285

Note: $d'_{99.5}$ and d'_{91} are obtained from cumulative number fractions and correspond very closely to d_{95} and d_{50}, respectively. The latter are obtained from data on cumulative volume fractions.

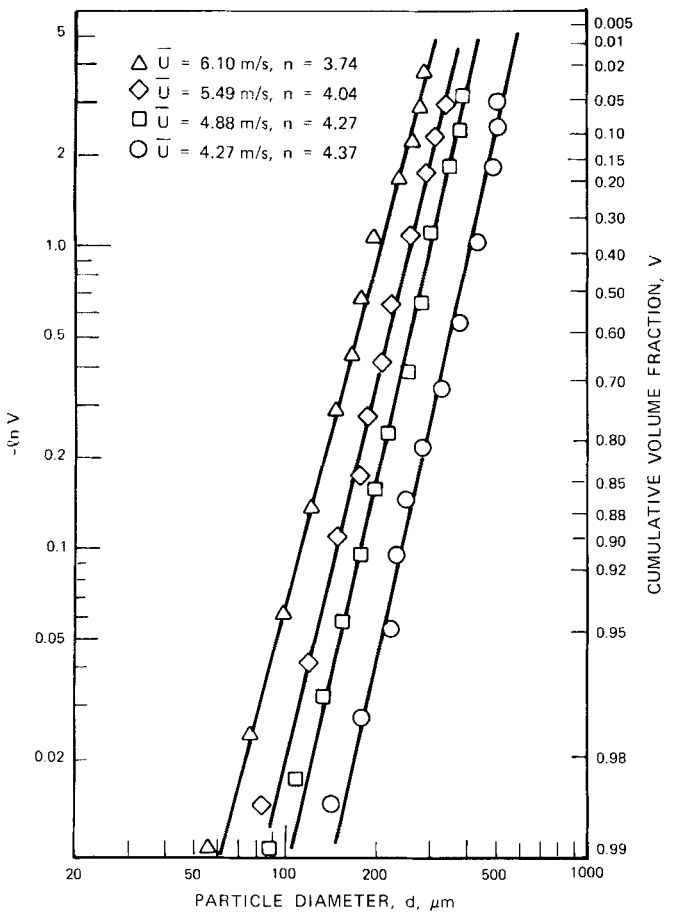

Fig. 12. Data by Collins (1967, p. 77). 1.3% light hydrocarbon dispersed in water.

recalled here that our data were obtained at ~590 pipe diameters downstream of the water injection point.

Collins concluded that none of the existing size distribution functions could satisfactorily describe his data. He did, however, recognize that the upper limit log-probability function gave the best fit. It was rejected, apparently for two reasons:

1. "A chi square test of the data for several systems indicated that in all cases the hypothesis that distribution obeyed the upper limit law could be rejected with only a 0.5% chance of error. The primary contribution to the chi square seemed to occur in the regions of largest and smallest drops" (Collins, 1967, p. 57).

2. The parameter d_{max} which gave the best fit using the upper limit function was considerably greater than d_{max} predicted by the Sleicher correlation.

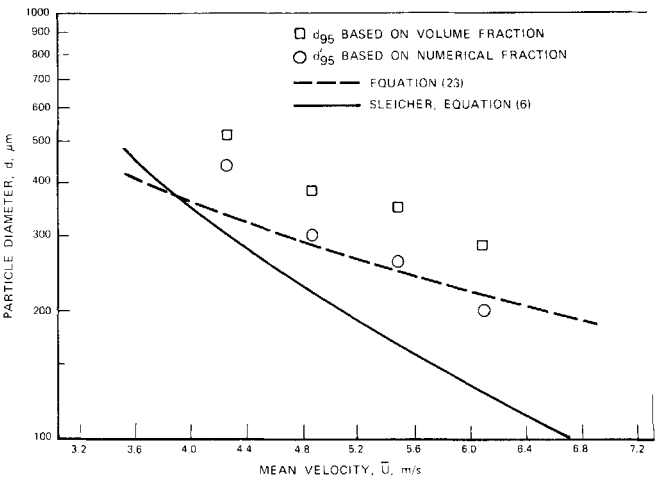

Fig. 13. Comparison of data by Collins (1967) with predicted maximum drop sizes.

The latter argument does not have any basis because the Sleicher correlation is empirical and probably inaccurate as shown in this study. With regard to the former argument, it is possible that very stringent criteria were used in statistically analyzing the data, as will become apparent below.

In order to compare the data reported by Collins with the results of this study, we have replotted several distributions using cumulative volume fractions instead of number frequencies. Figure 12 shows the only available data set taken at four different velocities, 421 pipe diameters from the injection point. Obviously, the Rosin-Rammler Equation (8) fits the data quite satisfactorily in the range $0.02 < V < 0.98$. A good fit is also obtained with the upper limit log-probability Equation (11).

The characteristic diameters d_{95} based on volume fractions and d'_{95} based on number frequencies are compared in Figure 13, with predictions obtained from Equation (23) and from Sleicher's correlation. The physical properties corresponding to these data are as follows: $t = 20°C$, $\mu_c \simeq 1.00$ mN s/m^2, $\sigma = 40.3$ mN/m, $\mu_d = 1.1$ mN s/m^2, $\rho_d = 0.782$ g/cm^3. Both correlations predict smaller than the measured d_{95}, but the modified Hinze correlation, Equation (23), is in better agreement with the data.

It will be noticed that the slope n of the distributions in Figure 12 is around 4.0, which is surprisingly close to the average slope obtained in our experiments with the same technique, that is, direct line photographs (see Table 3). This similarity may not be accidental. It is possible that Collins' photographic technique had the same drawbacks as ours, systematically favoring the larger droplets. This was shown in our case by comparison with the more accurate data obtained by means of the droplet encapsulation technique. If similar errors were involved in Collins' data, the maximum drop size, or d_{95}, obtained from the measured distributions would be greater than the true maximum size. This would also explain the discrepancy between data and predictions shown in Figure 13.

The results of the above comparisons can be summarized as follows:

1. Collins' data indicate that the test section length used in this study (~590 pipe diameters) is sufficient to form the maximum stable drop diameter.

2. Most of his data plotted in terms of cumulative volume fractions can be fitted with a Rosin-Rammler or an upper limit log-probability type of distribution function, as is the case with our data.

3. The characteristic slope of these distributions is high ($n \simeq 4$) and probably unrepresentative of the true size spectra.

4. Data on d_{95} appear to be in better agreement with the correlation proposed here than with Sleicher's correlation.

Manuscript received March 21, 1977; revision received October 26, and accepted October 27, 1977.